



# Aboveground biomass in Inner Mongolian temperate grasslands decreases under climate warming

Guocheng Wang<sup>1</sup>, Zhongkui Luo<sup>2</sup>, Yao Huang<sup>3</sup>, Wenjuan Sun<sup>3</sup>, Yurong Wei<sup>4</sup>, Xi Deng<sup>5</sup>, Jinhuan Zhu<sup>6</sup>, Wen Zhang<sup>1</sup>

- 5 <sup>1</sup>LAPC, Institute of Atmospheric Physics, Chinese Academy of Sciences, Beijing, 100029, China.  
<sup>2</sup>College of Environmental and Resource Sciences, Zhejiang University, Hangzhou 310058, Zhejiang, China.  
<sup>3</sup>State Key Laboratory of Vegetation and Environmental Change, Institute of Botany, Chinese Academy of Sciences, Beijing 100093, China.  
<sup>4</sup>Inner Mongolia Ecology and Agrometeorology Centre, Hohhot, Inner Mongolia 100051, China.  
10 <sup>5</sup>School of Atmospheric Sciences and Guangdong Province Key Laboratory for Climate Change and Natural Disaster Studies, Sun Yat-sen University, Zhuhai 519000, China  
<sup>6</sup>LAOR, Institute of Atmospheric Physics, Chinese Academy of Sciences, Beijing, 100029, China.

Correspondence to: Guocheng Wang (wanggc@mail.iap.ac.cn)

**Abstract.** Grassland aboveground biomass (AGB) is a critical component of the global carbon cycle and reflects ecosystem productivity. Although it is widely acknowledged that dynamics of grassland biomass are significantly regulated by climate change, *in situ* evidence at large spatiotemporal scales is limited. Here, we combine biomass measurements from six long-term (> 30 years) experiments and data in existing literatures to explore the spatiotemporal changes in AGB in Inner Mongolian temperate grasslands. We show that, on average, annual AGB over the past four decades is 2,561 kg ha<sup>-1</sup>, 1,496 kg ha<sup>-1</sup> and 835 kg ha<sup>-1</sup>, respectively, in meadow steppe, typical steppe and desert steppe in Inner Mongolia. The spatiotemporal changes of AGB are regulated by interactions of climatic attributes, edaphic properties, grazing intensity and grassland type. Using a machine learning-based approach, we map annual AGB (from 1981 to 2100) across the Inner Mongolian grassland at the spatial resolution of 1 km. We find that on the regional scale, meadow steppe has the highest annual AGB, followed by typical and desert steppe. During 1981-2019, the average annual AGB generally exhibited a declining trend across all the three types of grassland. Under future climate warming, AGB in the study region could continue to decrease. On average, compared with the historical AGB (i.e., average of 1981-2019), the AGB at the end of this century (i.e., average of 2080-2100) would decrease by 14% under RCP4.5 and 28% under RCP8.5, respectively. The decreases in AGB under warming show large disparities across different grassland types and future climate change scenarios. Our results demonstrate the accuracy of predictions in AGB using a machine learning-based approach driven by several readily obtainable environmental variables; and provide new data at large scale and fine resolution extrapolated from field measurements.

## 30 1 Introduction

Grassland occupies ~40% of the world land and is an essential component of global terrestrial ecosystems (Hufkens et al., 2016). Grassland provides plenty of ecosystem services such as supplying food to livestock therefore meat and milk to humans (Sattari et al., 2016) and accumulating carbon from atmosphere thus mitigating global warming (O'Mara, 2012). All of these



functions are more or less directly dependent on grassland biomass, which has been recognized significantly influenced by  
35 environmental changes and anthropogenic activities (Hovenden et al., 2019). Thus, quantifying the dynamics of grassland  
biomass and revealing underlying mechanisms, particularly at large extents of space and time, are of fundamental importance  
(Andresen et al., 2018).

Dynamics of grassland biomass are driven by complex interactions among a series of environmental attributes, among which  
climate is one of the most predominant drivers (De Boeck et al., 2008; Wang et al., 2020). The magnitudes and directions of  
40 climate change effects on AGB can vary across different local environments as well. In high altitude or latitude regions, climate  
warming can avail to biomass accumulation because of the reduced constraints of low temperature on plant growth (Park et  
al., 2019; Gonsamo et al., 2018). For example, using a data-model integration approach, Zeng et al. (2019) found that annual  
plant biomass was significantly and positively correlated with temperature in Tibetan Plateau. In the arid and semi-arid systems,  
however, warming can have harmful effects on biomass formation because warming can aggravate the negative effects of  
45 water limitation on plant growth (Fan et al., 2009; Hu et al., 2007).

Mean annual climate attributes (e.g., temperature and precipitation) have widely been treated as the potential drivers on  
spatiotemporal changes in grassland biomass (Fan et al., 2009; Ma et al., 2008). However, growing evidences have  
demonstrated the importance of seasonality and intra-annual variability of climate, rather than the mean annual climate  
attributes, in regulating the grassland biomass dynamics (Grant et al., 2014; Godde et al., 2020). These effects of seasonality  
50 and intra-annual variability in climates have seldom been considered in studies focusing on large spatial extents, e.g., Inner  
Mongolia, where China's largest temperate grassland locates in. It is noted that Inner Mongolian grassland accounts for more  
than half of China's northern temperate grassland area (Department of Animal Husbandry and Veterinary, 1996) and has the  
nation's largest grassland biomass carbon stock (Piao et al., 2004). The annual productivity of Inner Mongolian grassland,  
however, tends to vary in response to climate change (Bai et al., 2008). Since the start of 1980s, warming took place in many  
55 parts of Inner Mongolia (Wang et al., 2019). Under this warming, the spatiotemporal changes in grassland AGB, however, is  
still unclear. Although efforts have been taken to quantify AGB variations at the regional scale, these quantifications using  
mainly remote-sensing approaches generally show large disparities (Guo et al., 2016; Ma et al., 2010a; Long et al., 2010).  
Evidences from the datasets independent of remote sensing products may help to disentangle the mysterious spatiotemporal  
dynamics of AGB at the regional scale. Moreover, existing studies have seldom considered the possible co-regulating effects  
60 of soil properties (Jia et al., 2011; Bhandari and Zhang, 2019), grassland types and grazing intensity (Eldridge and Delgado-  
Baquerizo, 2017) on AGB, which might lead to large uncertainties and biases in these estimations. In addition, little is known  
about the consequences of the likely future climate change on AGB dynamics across time and space, which is a substantial  
concern in the context of global warming.

In this study, we collate to date the most comprehensive dataset of *in situ* measurements on plant biomass and climatic records  
65 in Inner Mongolian grassland from six long-term (more than 30 year) experiments and those data in the region from existing



literatures. We calibrate and validate a machine learning-based model for predicting the aboveground biomass in the study region, by treating tens of environmental covariates (climates, soils, grazing intensity, and grassland type) as predicting variables. Then, we map the annual aboveground biomass at a spatial resolution of 1 km in Inner Mongolian grassland over the periods of 1981-2019 (using historical climatic dataset) and 2020-2100 [using climate projections driven by two representative concentration pathways (e.g., RCP4.5 and RCP8.5)]. Based on the mapping products, finally, we analyse the spatiotemporal variations in AGB across the study area over the study periods.

## 2 Materials and Methods

### 2.1 Datasets of grassland aboveground biomass

In this study, we acquired two datasets of *in situ* aboveground biomass (AGB) in Inner Mongolian grassland. First, we obtained the AGB at six long-term (i.e., more than 30 years) experimental sites across the study region (Fig. 1a, Data S1). These six sites were established by Inner Mongolia Meteorological Bureau of China at early 1980s, measurements of AGB at each site has been carried out year by year since then. At each site, four fenced plots (i.e., four replicates) were set up to collect plant biomass data during plant growing seasons (e.g., from May to September). For each measurement replicate, the plants within a one square meter area were clipped and collected in a cloth bag. The samples were further air-dried to constant weights (weighted once every three days until the percent change in two consecutive weights are less than 2%). It is noted that plant growth rate could peak at different periods across time and space. Following Scurlock et al. (2002), we determined the annual plant biomass as the largest observed monthly biomass during a year (normally at the end of August at Ergun and at the end of September at other three sites). Apart from these six long-term field experiments, we also retrieved a dataset regarding grassland AGB from Xu et al. (2018), who recently conducted a thorough literature synthesis and obtained a comprehensive dataset of plant biomass in the grasslands of northern China. For the dataset constructed by Xu et al. (2018), in this study, we use only the observations conducted in Inner Mongolian grassland and with investigation time and coordinates clearly reported (Fig. 1a). In general, the Inner Mongolian grassland AGB derived from these two datasets (i.e., long-term experiments and literature synthesis) are comparable (Fig. S1). In total, we obtained 511 individual measurements across 247 locations in Inner Mongolian temperate grasslands (Fig. 1a, Data S1).

### 2.2 Environmental covariates

Environmental covariates including climate, soil, grassland type and grazing intensity were retrieved for both AGB driver assessment and model fitting. For climatic covariates, we first obtained the daily climatic records of 120 climatic stations established in Inner Mongolia (Fig. 1b) from the National Meteorological Information Centre (NMIC) of China. The daily climatic attributes such as minimum, average and maximum temperature and precipitation were transformed into monthly time series data using the *daily2monthly* function in the R package *hydroTSM*. Based on these monthly data, we calculated 23 bioclimatic variables (Table S1) with an annual time step over the period of 1981-2019 by using the *biovars* function in the R



package *dismo*. By doing so, we aim to comprehensively consider the possible effects of seasonality, intra- and inter-annual variability of climates (Fick and Hijmans, 2017). By further applying an interpolation algorithm (Thornton et al., 1997) to these 23 bioclimatic variables at the 120 stations, we created the raster layers of the climatic attributes with a spatial resolution of 1 km year by year. For the edaphic covariates, we directly extracted 10 raster soil layers representing key soil physical and chemical properties (Table S1) at a 1 km spatial resolution in the study region from ISRIC-WISE soil profile database (Batjes, 2016).

The grazing intensity in this study was represented by the quantity of three key animals (i.e., cattle, sheep and goats; Table S1) because they are the majority in Inner Mongolian grasslands (National Bureau of Statistics of China, 1981-2019). Here, we first derived the regional distribution data for cattle (Fig. S2 a), goat (Fig. S2 b) and sheep (Fig. S2 c) during 2010 in the study region from Gilbert et al. (2018). Then, we obtained the yearly total amount of each livestock in the study region (Fig. S2 d) from National Bureau of Statistics of China (1981-2019). By assuming a similar spatial distribution of livestock over time, we generated raster layers of each of the three animals year by year over the past four decades using the above-mentioned two datasets. In addition, a spatial layer of grassland type (i.e., meadow steppe, typical steppe and desert steppe; Fig. 1a and Table S1) at 1 km resolution was derived from the Vegetation Map of China (Zhang, 2007), the digital version of which is publicly obtainable (<http://data.casearth.cn/sdo/detail/5c19a5680600cf2a3c557b6b>).

### 2.3 Machine learning models to predict grassland biomass

To predict grassland aboveground biomass (AGB) across the region, we generated a suite of machine learning-based predictive models for AGB, treating edaphic, climatic, grassland type and grazing intensity (Table S1) as candidate predictors. Here, data from the 511 measurements (Fig. 1a and Data S1) were used to fit the models. For the spatial layers of soil properties and grassland type, which were assumed to be constant over time, we retrieved the associated covariates using the geographical coordinates of the 511 measurements. For those variables varying over time (e.g., climatic variables and grazing intensities), we extracted the associated attributes using both the locations and investigating year of the 511 measurements. In fitting the models, AGB is treated as a dependent variable and the environmental covariates (Table S1) are treated as independent variables. Before fitting the models, we converted the categorical variables (i.e., grassland type) to dummy variables. Then, the function *findCorrelation* in R package *caret* was used to exclude the environmental covariates with high multicollinearities. The remaining attributes were further adopted in model training (80% stratified samples) and validation (the remaining 20% stratified samples). We used a 10-fold cross-validation to train a suite of machine learning models using three algorithms [i.e., random forest (RF), Cubist and support vector machines (SVM)], which are implemented in the R package *caret*. The amount of variance in AGB explained by each model was assessed by the coefficient of determination ( $R^2$ ). The root mean square error (RMSE) was also calculated to compare the model simulations and observations. Apart from the three individual models, we also derived an ensemble model by adopting a principal component analysis (PCA) approach based on the predictions of



the three algorithms. In brief, the smaller an individual model's RMSE is, the more the model's output contributes to final predictions.

## 130 2.4 Assessment of drivers on AGB

The machine learning models themselves provide assessments of the relative importance (RI) of each independent variable in predicting the dependent variable (e.g., grassland AGB in this study). In general, the greater the RI of a variable is, the larger its influence on AGB is. We also adopted the Mantel test (Mantel, 1967) to assess the relationship between similarity of different grassland types and the similarity of environmental covariates. Here, the standardized Mantel's  $r$  (ranges from 0 to 1) is used to represent the strength of this relationship (the higher the Mantel's  $r$  is, the stronger the correlation is) and the associated significance is indicated by the  $p$  value determined from 999 randomization (Legendre and Fortin, 1989). Here, the R package *vegan* is used to perform the Mantel test.

## 2.5 Regional mapping and uncertainty analysis

Using the fitted machine learning-based ensemble model, we mapped AGB in Inner Mongolian grassland (at a spatial resolution of 1 km) on an annual time step in the history and future. In mapping the historical AGB (i.e., during 1981-2019), the model is run using environmental covariates extracted from the regional data layers (see *Environmental covariates*). Prediction uncertainty was quantified using a Monte Carlo analysis to develop the probability density functions (PDF) for each edaphic, climatic and livestock variable within the ranges of mean  $\pm 10\%$ . The ensemble machine learning model was then run for 200 times in each grid with each of independent variables assigned from the PDF. The average and coefficient variation (CV, calculated as the standard deviation divided by the average) were then determined in each grid using the 200 model outputs to represent the predicted AGB and the associated uncertainty, respectively.

For predictions of AGB in the future (i.e., 2020-2100), we include the climatic datasets projected by one typical CMIP5 global circulation model (GCM) to save computing resources. In this study, we use the projections output by CESM1-BGC, which was run by National Center for Atmospheric Research (NCAR). Here, we directly obtained the processed climatic products constructed by Karger et al. (2020), who recently generated a downscaled and bias-corrected temperature and precipitation datasets. Specifically, these future climatic datasets were driven by two scenarios of representative concentration pathways (RCP4.5 and RCP8.5) at monthly step in this century. According to the model projections, mean annual temperature (MAT) under both RCPs will continue to increase in the following decades (Fig. S3). The extent of climate warming is generally higher under RCP8.5 than that under RCP4.5 (Fig. S3). After obtaining the future climate datasets, we also use the *biovars* function in R environment (see *Environmental covariates*) to calculate the 23 interested bioclimatic attributes (Table S1) for both scenarios of RCPs year by year from 2020 to 2100. In projecting the future AGB dynamics using the ensemble machine learning model, we assume that the soil properties will not significantly change over time (i.e., the same soil inputs used in historical AGB predictions) and current grazing intensity will keep relatively stable (i.e., the average of the recent five years).



In addition, the uncertainty analysis for future AGB predictions were performed using the same approach as that adopted in  
160 mapping the historical AGB. All statistical analyses and graphical productions in this study were performed in R v3.6.3 (R  
Development Core Team, 2020).

### 3 Results

The field observations indicate that, on average, aboveground biomass (AGB) in Inner Mongolian grassland is  $1,700 \text{ kg ha}^{-1}$   
ranging from  $220 \text{ kg ha}^{-1}$  [2.5% confidence intervals (CI)] to  $4,827 \text{ kg ha}^{-1}$  (97.5% CI, Fig. 2). Across the three grassland types,  
165 meadow steppe has the highest AGB ( $2,561 \text{ Mg ha}^{-1}$  ranging from  $736 \text{ Mg ha}^{-1}$  to  $5,537 \text{ Mg ha}^{-1}$ ), followed by typical steppe  
( $1,496 \text{ Mg ha}^{-1}$  ranging from  $213 \text{ Mg ha}^{-1}$  to  $4,418 \text{ Mg ha}^{-1}$ ), and desert steppe has the lowest AGB ( $835 \text{ Mg ha}^{-1}$  ranging from  
 $234 \text{ Mg ha}^{-1}$  to  $1,928 \text{ Mg ha}^{-1}$ , Fig. 2).

The fitted three individual machine learning algorithms (i.e., RF, Cubist and SVM) can explain overall 32%-48% of the  
variance in observed AGB (Fig. 3a, b and c). The ensemble model of the three algorithms can better simulate the observations  
170 than any of those individual models (Fig. 3). On average, 52% of the variance in the observations can be explained by the  
ensemble model (Fig. 3d). Although the variable importance differed among the three algorithms, climatic and livestock  
variables seem to substantially affect the AGB dynamics (Fig. S4). After excluding the covariates with high multilinearities,  
the remaining 10 climatic attributes, 5 edaphic variables and three livestock predictors generally show small autocorrelations  
(Fig. 4). Mantel test suggests that, compared to the edaphic and livestock attributes, the climatic variables are in general  
175 stronger correlators of AGB in the three grassland types (Fig. 4).

The regional mapping results of grassland AGB during 1981-2019 show large spatial variations (Fig. 5a). On average, the  
regional AGB during the past four decades is  $1,438 \text{ kg ha}^{-1}$ , the corresponding lower and upper limits of the 95% CI is  $479 \text{ kg}$   
 $\text{ha}^{-1}$ , and  $2,284 \text{ kg ha}^{-1}$ , respectively (Fig. 5a). Across grassland types, meadow steppe has the highest average AGB ( $2,194 \text{ Mg}$   
 $\text{ha}^{-1}$  ranging from  $1,153 \text{ Mg ha}^{-1}$  to  $2,631 \text{ Mg ha}^{-1}$ ), followed by typical steppe ( $1,552 \text{ Mg ha}^{-1}$  ranging from  $539 \text{ Mg ha}^{-1}$  to  
180  $2,200 \text{ Mg ha}^{-1}$ ) and desert steppe ( $893 \text{ Mg ha}^{-1}$  ranging from  $405 \text{ Mg ha}^{-1}$  to  $1,341 \text{ Mg ha}^{-1}$ , Fig. 5a). Spatially, the average  
coefficient of variation (CV) in the predictions is lowest in meadow steppe (10.5%), followed by desert steppe (14.6%) and  
typical steppe (21.8%, Fig. 5d). Over 1981-2019, the regional average AGB displayed a decreasing trend in the first three  
decades and then kept relatively stable in the recent decade (Fig. 6a). Among the three grassland types, the historical changes  
in AGB (Fig. 6b, c and d) are in general consistent with that of the total Inner Mongolian grassland AGB (Fig. 6a).

185 Our predicting results show that future AGB in general decreases under both scenarios of RCPs (i.e., RCP4.5 and RCP8.5, Fig.  
5 and Table 1). Compared with the historical AGB (i.e., average AGB during 1981-2019, hereafter the same), on average,  
AGB at the end of this century (i.e., average of 2080-2100, hereafter the same) would decrease by 14% under RCP4.5 (Fig.  
5b) and 28% under RCP8.5, respectively (Table 1). The decreases in AGB under climate change show large disparities across



different grassland types and climate change scenarios. Compared with the historical average AGB, AGB at the end of this century under RCP4.5 is estimated to decrease by a smaller extent (i.e., 10%) in meadow steep than those in typical (16%) and desert steep (21%, Table 1). In general, AGB under RCP8.5 would reduce by larger extents compared with those under RCP4.5. Under RCP8.5, the average AGB at the end of this century is estimated to experience a 24% (in meadow steep), 30% (in typical steep) and 25% (in desert steep) reduction, compared with the averages over 1981-2019 (Table 1). The magnitudes and spatial patterns of CV in the simulations under both RCP4.5 (Fig. 5e) and RCP8.5 (Fig. 5f) are comparable with those during the period of 1981-2019 (Fig. 5d).

#### 4 Discussion

Our results, based on AGB observations derived from six long-term field experiments and literature synthesis, indicate the large spatial disparities in aboveground biomass across different grassland types (Fig. 2). This gradient spatial pattern in AGB, i.e., largest in meadow steep followed by that in typical and desert steep, is comparable with Ma et al. (2008), who carried out a comprehensive field measurements and investigated 113 locations in Inner Mongolian temperate grassland during 2002-2005. On the regional scale, we mapped grassland AGB at high spatial and temporal resolutions, which shows that AGB generally decreases from north-eastern to south-western areas in the study region (Fig. 5a). Such a spatial pattern is also consistent with the maps generated from remote sensing derivations (Fig. S5). This demonstrates the accuracy of our machine learning model's predictions. It should be noted that existing mapping products of grassland AGB use mainly remote sensing approaches requiring inputs from satellite-based datasets (Guo et al., 2016; Ma et al., 2010a; Jiao et al., 2019). Our fitted machine learning model, however, uses only several readily obtainable environmental covariates (Fig. 4 and Table S1). Our results demonstrate the ability of machine learning approach to effectively extrapolate grassland AGB to much larger spatiotemporal extents (e.g., Fig. 5 and 6).

Our simulation results show that, under the climate warming over the past four decades (Fig. S3), the average AGB generally experienced a declining trend across all the three grassland types in Inner Mongolia (Fig. 6). This demonstrates the possible negative effect of temperature rising on AGB that has been widely reported (De Boeck et al., 2008; Wang et al., 2020), particularly in the arid and semi-arid ecosystems (Ma et al., 2010b). This harmful influence of warming on AGB is explainable. For example, in a system restrained by water availability (e.g., temperate grassland), warming can not only inhibit plant photosynthesis (Xu and Zhou, 2005) but also enhance evaporation and further intensify water stress (De Boeck et al., 2006) thereby decreasing grassland biomass. Precipitation has generally been recognized to have positive effects on AGB in the temperate grassland (Hovenden et al., 2019; Ma et al., 2010a), which supports our findings in this study. For example, the simulated average AGB is relatively higher in the years with higher MAP (e.g., 1998 and 2012) than those in other years (Fig. 6a). The importance of precipitation on AGB can be more reflected by the spatial patterns of these two attributes, e.g., AGB is much lower in the more arid regions (Fig. 5a) where soils are suffering severer water deficiencies. Apart from climatic



220 factors, our results also demonstrate the regulating effects of soil conditions and livestock on the dynamics of grassland AGB (Fig. 4 and S4). This is consistent with several findings highlighting the importance of soil physical and chemical characteristics (Yang et al., 2009; Griffiths et al., 2012) and grazing intensity (Eldridge and Delgado-Baquerizo, 2017) in controlling grassland biomass changes.

We notice that our model predictions show larger interannual variations in AGB (Fig. 6a) than those in the estimations based on remote sensing approaches (Fig. S5). In fact, the remote sensing derived AGB has also been bias-corrected by the field measurements (Jiao et al., 2019). Consequently, this disparity could be related to the difference of observed AGB datasets used in different studies. Specifically, the measurements of biomass used to calibrate remote-sensing data [normalized difference vegetation index (NDVI)] in Jiao et al. (2019) were generally conducted during 2001-2015. Extrapolations of these observations from a short term (e.g., 2001-2015) to a much longer term (e.g., 1982-2015) might lead to underestimations in the long-term interannual variabilities. Our study, however, integrate the *in situ* observed data from six long-term (1982-2015) field experiments (Fig. 1a), which can potentially reduce the possible biases in model predictions. In addition, we find that the overall decrease in Inner Mongolian grassland biomass are contributed greater by the decline during the first three decades and the declining trend in AGB seems to be alleviated in the recent decade (Fig. 6). This could be related to the overall slowing climate warming over the recent decade (Fig. S3). In the future, a faster warming (e.g., RCP8.5) climate will lead to a larger reduction in grassland AGB (Fig. 5b and c). It is noteworthy that the accuracy of our predictions on future grassland AGB relies substantially on the robustness of future climate change projections simulated by the GCMs (e.g., CESM1-BGC). However, although CESM1-BGC (like all other CMIP5 models) can reasonably well simulate changes in temperature, it may not well predict precipitation, particularly for Eastern China where is strongly affected by large-scale atmospheric circulations (Huang et al., 2013). Consequently, it should be cautious in interpreting the likely decrease of AGB under future temperature rising (Fig. 6), because the large uncertainties in projected precipitation may lead to biased predictions in AGB.

## 5 Conclusions

Our results demonstrate that the aboveground biomass in Inner Mongolian grasslands shows large spatial and temporal variations during the past four decades, which is driven by a series of environmental covariates. Particularly, current climate change characterized mainly by warming has negative effects on AGB across all types of grassland. In addition, our results demonstrate that adopting a machine learning model approach with only a few readily obtainable environmental predictors can accurately capture AGB dynamics, which enables extrapolations of AGB across larger spatiotemporal extents. Moreover, our study provides new data on annual AGB in the study region at fine spatial (1km) and temporal (yearly) resolutions for both historical (1981-2019) and future (2020-2100) periods under different climate change scenarios.

**Data availability.** The data that support the findings of this study (Data S1) are openly available at: 10.6084/m9.figshare.13108430.





**Supplement.** The supplement related to this article is available online at: XXX.

**Author contributions.** G. Wang and Y. Huang conceived this study. G. Wang conducted the data analysis with interpretations from Z. Luo and Y. Huang. G. Wang and Z. Luo prepared the article with contributions from all co-authors.

**Competing interests.** The authors declare that they have no conflict of interest.

255 **Acknowledgements.** The authors acknowledge the people who conducted the filed long-term experiments and collected the observed data.

**Financial support.** This study is financially supported by the National Natural Science Foundation of China (Grant No. 41590875, 41775156).

## References

- 260 Andresen, L. C., Yuan, N., Seibert, R., Moser, G., Kammann, C. I., Luterbacher, J., Erbs, M., and Müller, C.: Biomass responses in a temperate European grassland through 17 years of elevated CO<sub>2</sub>, *Global Change Biol*, 24, 3875-3885, 2018.
- Bai, Y., Wu, J., Xing, Q., Pan, Q., Huang, J., Yang, D., and Han, X.: Primary production and rain use efficiency across a precipitation gradient on the Mongolia plateau, *Ecology*, 89, 2140-2153, 2008.
- Batjes, N. H.: Harmonized soil property values for broad-scale modelling (WISE30sec) with estimates of global soil carbon stocks, *Geoderma*, 269, 61-68, 10.1016/j.geoderma.2016.01.034, 2016.
- 265 Bhandari, J., and Zhang, Y.: Effect of altitude and soil properties on biomass and plant richness in the grasslands of Tibet, China, and Manang District, Nepal, *Ecosphere*, 10, e02915, 10.1002/ecs2.2915, 2019.
- De Boeck, H. d., Lemmens, C., Zavalloni, C., Gielen, B., Malchair, S., Carnol, M., Merckx, R., Van den Berge, J., Ceulemans, R., and Nijs, I.: Biomass production in experimental grasslands of different species richness during three years of climate warming, *Biogeosciences*, 585-594, 2008.
- 270 De Boeck, H. J., Lemmens, C. M., Bossuyt, H., Malchair, S., Carnol, M., Merckx, R., Nijs, I., and Ceulemans, R.: How do climate warming and plant species richness affect water use in experimental grasslands?, *Plant Soil*, 288, 249-261, 2006.
- Department of Animal Husbandry and Veterinary: Rangeland resources of China, China Science and Technology Press Beijing (in Chinese), 1996.
- 275 Eldridge, D. J., and Delgado-Baquerizo, M.: Continental-scale impacts of livestock grazing on ecosystem supporting and regulating services, *Land Degradation & Development*, 28, 1473-1481, 2017.
- Fan, J., Wang, K., Harris, W., Zhong, H., Hu, Z., Han, B., Zhang, W., and Wang, J.: Allocation of vegetation biomass across a climate-related gradient in the grasslands of Inner Mongolia, *J Arid Environ*, 73, 521-528, 2009.
- Fick, S. E., and Hijmans, R. J.: WorldClim 2: new 1-km spatial resolution climate surfaces for global land areas, *Int J Climatol*, 37, 4302-4315, 10.1002/joc.5086, 2017.
- 280 Gilbert, M., Nicolas, G., Cinardi, G., Van Boeckel, T. P., Vanwambeke, S. O., Wint, G. W., and Robinson, T. P.: Global distribution data for cattle, buffaloes, horses, sheep, goats, pigs, chickens and ducks in 2010, *Scientific data*, 5, 1-11, 2018.
- Godde, C. M., Boone, R., Ash, A. J., Waha, K., Sloat, L., Thornton, P. K., and Herrero, M.: Global rangeland production systems and livelihoods at threat under climate change and variability, *Environmental Research Letters*, 15, 044021, 2020.
- 285 Gonsamo, A., Chen, J. M., and Ooi, Y. W.: Peak season plant activity shift towards spring is reflected by increasing carbon uptake by extratropical ecosystems, *Global Change Biol*, 24, 2117-2128, 2018.
- Grant, K., Kreyling, J., Dienstbach, L. F., Beierkuhnlein, C., and Jentsch, A.: Water stress due to increased intra-annual precipitation variability reduced forage yield but raised forage quality of a temperate grassland, *Agriculture, Ecosystems & Environment*, 186, 11-22, 2014.
- 290 Griffiths, B. S., Spilles, A., and Bonkowski, M.: C:N:P stoichiometry and nutrient limitation of the soil microbial biomass in a grazed grassland site under experimental P limitation or excess, *Ecological Processes*, 1, 6, 10.1186/2192-1709-1-6, 2012.
- Guo, L. H., Hao, C. Y., Wu, S. H., Zhao, D. S., and Gao, J. B.: Analysis of changes in net primary productivity and its susceptibility to climate change of Inner Mongolian grasslands using the CENTURY model, *Geographical Research*, 35, 271-284 (in Chinese with English abstract), 2016.
- 295 Hovenden, M. J., Leuzinger, S., Newton, P. C., Fletcher, A., Fatichi, S., Lüscher, A., Reich, P. B., Andresen, L. C., Beier, C., and Blumenthal, D. M.: Globally consistent influences of seasonal precipitation limit grassland biomass response to elevated CO<sub>2</sub>, *Nature plants*, 5, 167-173, 2019.

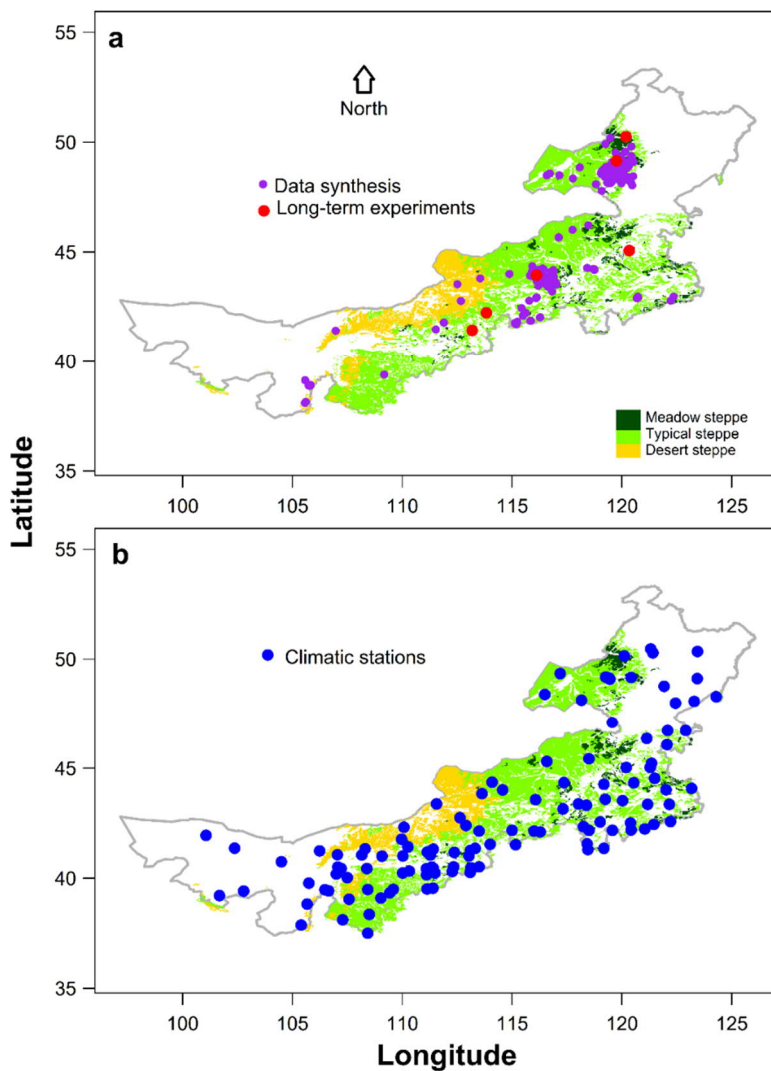


- Hu, Z., Fan, J., Zhong, H., and Yu, G.: Spatiotemporal dynamics of aboveground primary productivity along a precipitation gradient in Chinese temperate grassland, *Sci China Ser D*, 50, 754-764, 10.1007/s11430-007-0010-3, 2007.
- 300 Huang, D.-Q., Zhu, J., Zhang, Y.-C., and Huang, A.-N.: Uncertainties on the simulated summer precipitation over Eastern China from the CMIP5 models, *Journal of Geophysical Research: Atmospheres*, 118, 9035-9047, 10.1002/jgrd.50695, 2013.
- Hufkens, K., Keenan, T. F., Flanagan, L. B., Scott, R. L., Bernacchi, C. J., Joo, E., Brunsell, N. A., Verfaillie, J., and Richardson, A. D.: Productivity of North American grasslands is increased under future climate scenarios despite rising aridity, *Nature Climate Change*, 6, 710-714, 2016.
- 305 Jia, X., Shao, M., Wei, X., Horton, R., and Li, X.: Estimating total net primary productivity of managed grasslands by a state-space modeling approach in a small catchment on the Loess Plateau, China, *Geoderma*, 160, 281-291, <https://doi.org/10.1016/j.geoderma.2010.09.016>, 2011.
- Jiao, C. C., YU, G. R., Chen, Z., and He, N. P.: A dataset for aboveground biomass of the northern temperate and Tibetan Plateau alpine grasslands in China, based on field investigation and remote sensing inversion (1982–2015), *China Scientific Data*, 4, DOI: 10.11922/csdata.2018.0029.zh, 2019.
- 310 Karger, D. N., Schmatz, D. R., Dettling, G., and Zimmermann, N. E.: High-resolution monthly precipitation and temperature time series from 2006 to 2100, *Scientific Data*, 7, 248, 10.1038/s41597-020-00587-y, 2020.
- Legendre, P., and Fortin, M. J.: Spatial pattern and ecological analysis, *Vegetatio*, 80, 107-138, 1989.
- Long, L. H., Li, X. B., Wang, H., Wei, D. D., and Zhang, C.: Net primary productivity (NPP) of grassland ecosystem and its relationship with climate in Inner Mongolia, *Acta Ecologica Sinica*, 30, 1367-1378 (in Chinese with English abstract), 2010.
- 315 Ma, W., Yang, Y., He, J., Zeng, H., and Fang, J.: Above-and belowground biomass in relation to environmental factors in temperate grasslands, Inner Mongolia, *Science in China Series C: Life Sciences*, 51, 263-270, 2008.
- Ma, W., Fang, J., Yang, Y., and Mohammad, A.: Biomass carbon stocks and their changes in northern China's grasslands during 1982–2006, *Science China Life Sciences*, 53, 841-850, 2010a.
- Ma, W., Liu, Z., Wang, Z., Wang, W., Liang, C., Tang, Y., He, J.-S., and Fang, J.: Climate change alters interannual variation of grassland aboveground productivity: evidence from a 22-year measurement series in the Inner Mongolian grassland, *Journal of Plant Research*, 123, 509-517, 10.1007/s10265-009-0302-0, 2010b.
- Mantel, N.: The detection of disease clustering and a generalized regression approach, *Cancer research*, 27, 209-220, 1967.
- O'Mara, F. P.: The role of grasslands in food security and climate change, *Ann Bot-london*, 110, 1263-1270, 2012.
- 325 Park, T., Chen, C., Macias-Fauria, M., Tømmervik, H., Choi, S., Winkler, A., Bhatt, U. S., Walker, D. A., Piao, S., and Brovkin, V.: Changes in timing of seasonal peak photosynthetic activity in northern ecosystems, *Global Change Biol*, 25, 2382-2395, 2019.
- Piao, S., Fang, J., He, J., and Xiao, Y.: Spatial distribution of grassland biomass in China, *Acta Phytocologica Sinica*, 28, 491-498(in Chinese with English Abstract), 2004.
- Sattari, S., Bouwman, A., Rodriguez, R. M., Beusen, A., and Van Ittersum, M.: Negative global phosphorus budgets challenge sustainable intensification of grasslands, *Nature communications*, 7, 1-12, 2016.
- 330 Scurlock, J. M., Johnson, K., and Olson, R. J.: Estimating net primary productivity from grassland biomass dynamics measurements, *Global Change Biology*, 8, 736-753, 2002.
- Thornton, P. E., Running, S. W., and White, M. A.: Generating surfaces of daily meteorological variables over large regions of complex terrain, *Journal of Hydrology*, 190, 214-251, 1997.
- 335 Wang, G., Huang, Y., Wei, Y., Zhang, W., Li, T., and Zhang, Q.: Climate Warming Does Not Always Extend the Plant Growing Season in Inner Mongolian Grasslands: Evidence From a 30-Year In Situ Observations at Eight Experimental Sites, *Journal of Geophysical Research: Biogeosciences*, 124, 2364-2378, 10.1029/2019jg005137, 2019.
- Wang, H., Liu, H., Cao, G., Ma, Z., Li, Y., Zhang, F., Zhao, X., Zhao, X., Jiang, L., and Sanders, N. J.: Alpine grassland plants grow earlier and faster but biomass remains unchanged over 35 years of climate change, *Ecol Lett*, 701-710, 10.1111/ele.13474, 2020.
- 340 Xu, L., Yu, G., He, N., Wang, Q., Gao, Y., Wen, D., Li, S., Niu, S., and Ge, J.: Carbon storage in China's terrestrial ecosystems: A synthesis, *Scientific reports*, 8, 1-13, 2018.
- Xu, Z., and Zhou, G.: Effects of water stress and high nocturnal temperature on photosynthesis and nitrogen level of a perennial grass *Leymus chinensis*, *Plant Soil*, 269, 131-139, 2005.
- Yang, Y., Fang, J., Pan, Y., and Ji, C.: Aboveground biomass in Tibetan grasslands, *J Arid Environ*, 73, 91-95, 2009.
- 345 Zeng, N., Ren, X., He, H., Zhang, L., Zhao, D., Ge, R., Li, P., and Niu, Z.: Estimating grassland aboveground biomass on the Tibetan Plateau using a random forest algorithm, *Ecological Indicators*, 102, 479-487, 2019.
- Zhang, X.: *Vegetation Map of China and Its Geographic Pattern: Illustration of the Vegetation Map of the People's Republic China (1: 10,000,000)*, Geological Press. 296–326., Beijing, 2007.

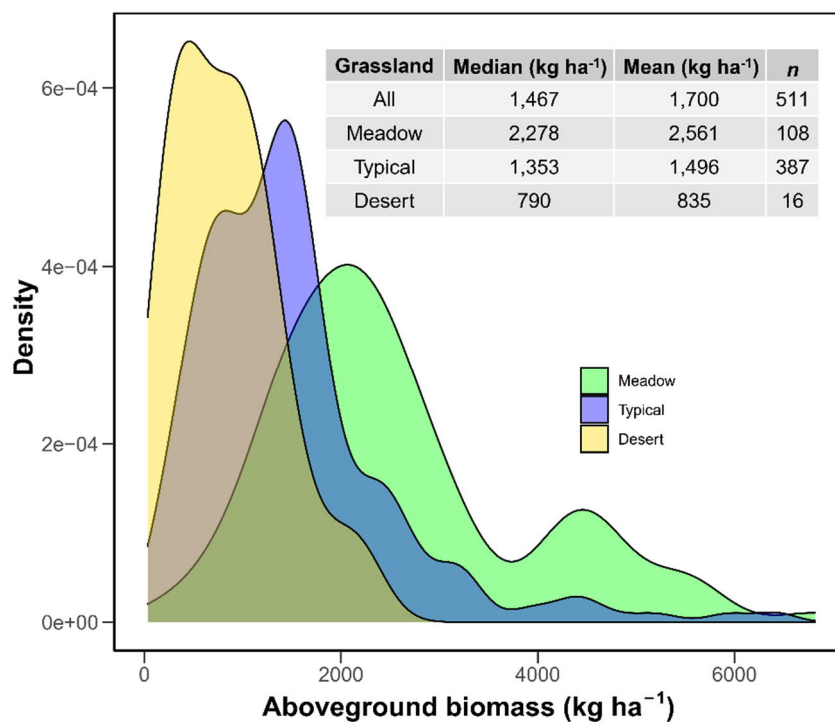


350 **Table 1 Summary of Inner Mongolian grassland aboveground (AGB) biomass during different periods**

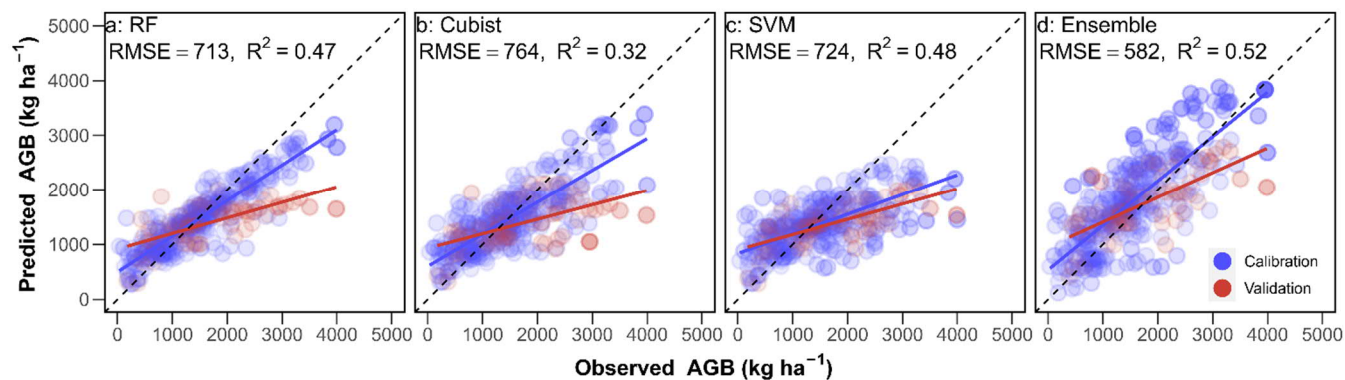
Category	Period	AGB across grassland types (kg ha <sup>-1</sup> , mean±SD)			
		Meadow	Typical	Desert	All
Historical	1981–1999	2,335±136	1,764±230	1,089±235	1,651±233
	2000–2019	2,059±171	1,350±214	706±263	1,236±221
Scenario RCP4.5	1981–2019	2,194±207	1,552±303	893±313	1,438±307
	2020–2039	1,934±112	1,345±201	918±287	1,304±181
	2040–2059	1,837±171	1,223±235	768±340	1,174±249
	2060–2079	1,916±117	1,312±184	779±275	1,253±191
	2080–2100	1,965±97	1,306±170	702±279	1,237±181
Scenario RCP8.5	2020–2039	1,902±107	1,269±156	740±294	1,206±163
	2040–2059	1,862±142	1,230±245	733±304	1,165±252
	2060–2079	1,800±123	1,219±193	722±308	1,169±202
	2080–2100	1,672±140	1,087±156	666±236	1,033±162



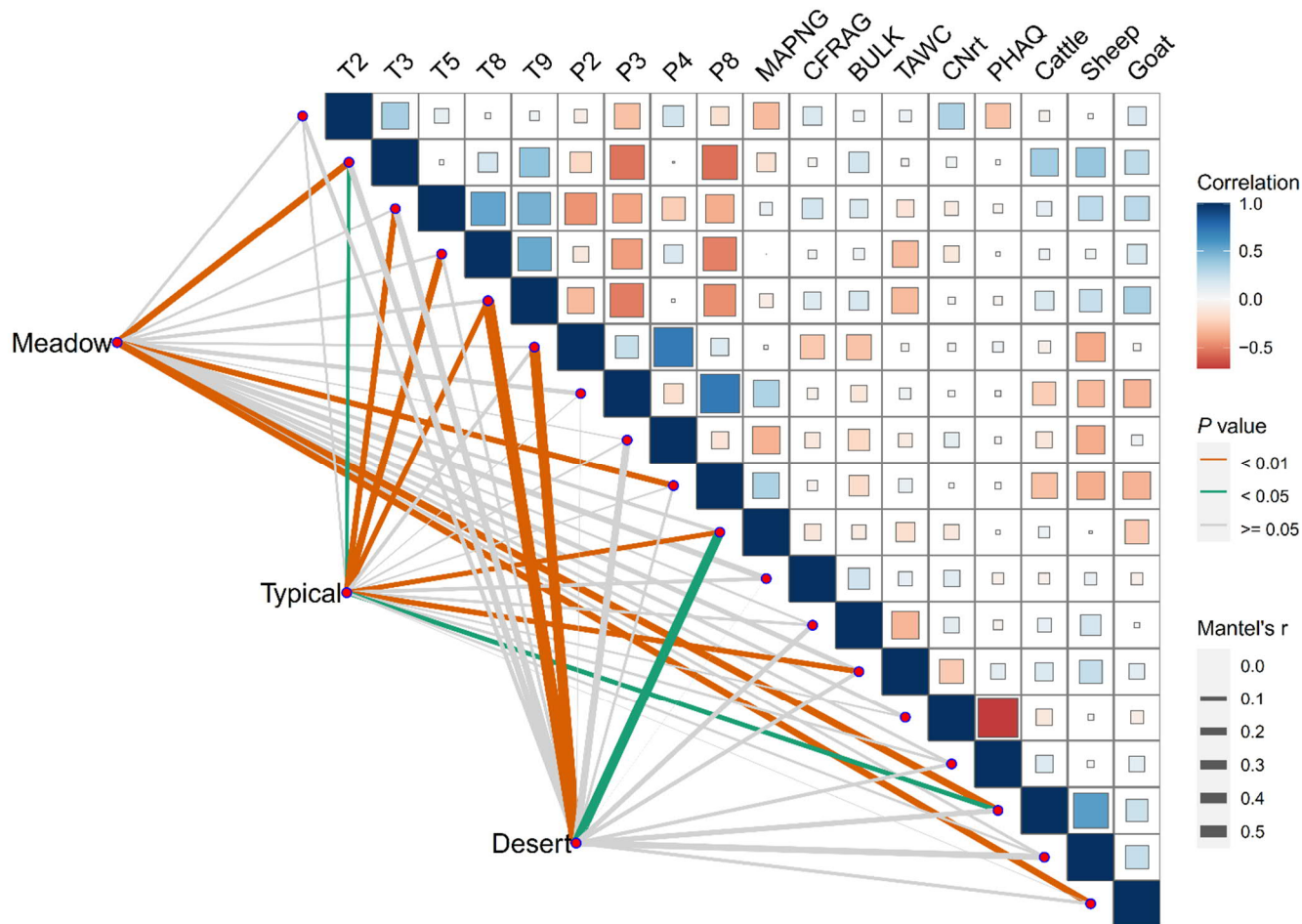
355 **Figure 1. Spatial distribution of grassland aboveground biomass observations (a) and the 120 climatic stations (b) in Inner Mongolia.** The Inner Mongolian grasslands are grouped into three categories (i.e., meadow steppe, typical steppe and desert steppe). Observations of grassland biomass are both derived from literature synthesis and the six long-term experimental sites. The ground climatic records are obtained from China's national meteorological bureau.



360 **Figure 2.** Aboveground biomass distribution across different grassland types in Inner Mongolia. See Fig. 1 for the spatial distribution of the three grassland types in Inner Mongolia.



365 **Figure 3. Performance of fitted machine learning-based models to predict grassland aboveground biomass (AGB).** a, random forest (RF); b, Cubist; c, support vector machines (SVM); d, the ensemble model of a-c. For each individual model, 80% of the stratified samples of observations were used for model calibration, with the other 20% used for validation.  $R^2$  and RMSE show the coefficient of determination and root mean square error of model validations.



370 **Figure 4. Environmental drivers of Inner Mongolian grassland biomass.** The upper triangle shows the pairwise comparisons of predicting variables, with a color gradient denoting Spearman's correlation coefficient. Taxonomic grassland type (i.e., meadow, typical and desert steppe) was related to each environmental factor by partial (geographic distance-corrected) Mantel test. Line color represents the statistical significance and line width denotes the Mantel's  $r$  statistic for the corresponding distance correlations. See Table S1 for descriptions of each variables.



375

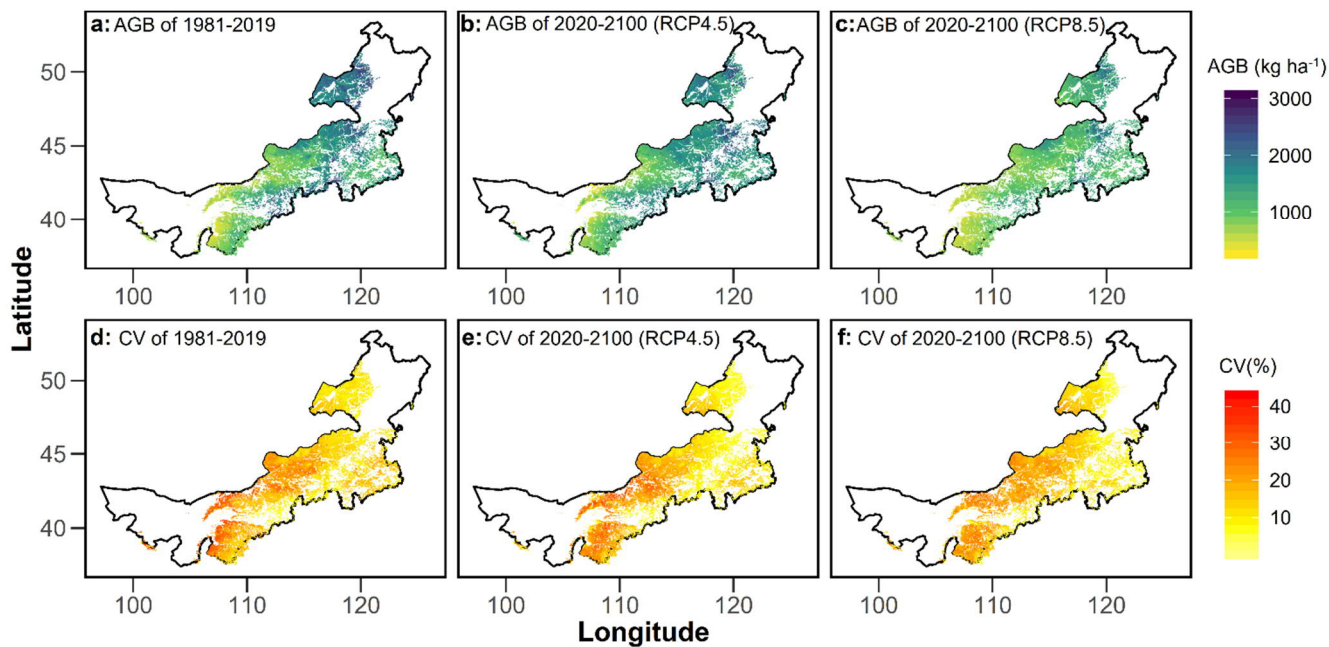
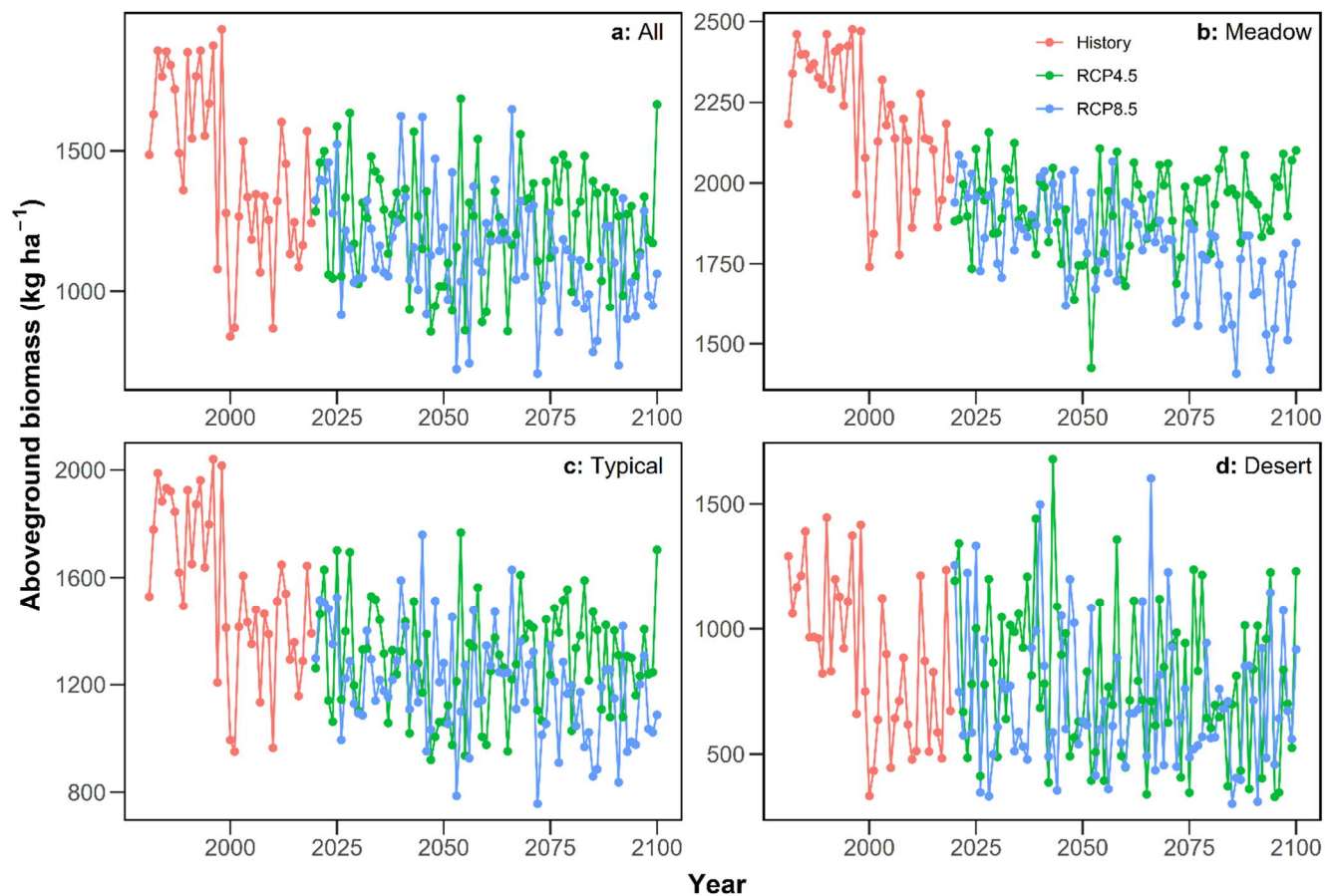


**Figure 5. Spatial patterns of Inner Mongolian grassland aboveground biomass (AGB) and the uncertainties in terms of coefficient of variations (CV).** The upper panel shows the average gridded AGB over 1981-2019 (a) and under two climate change scenarios [RCP4.5 (b) and RCP8.5 (c)] over 2020-2100. The lower panel (d, e and f) exhibit the associated CV of the upper panel.





380

**Figure 6.** Temporal variations of the average aboveground biomass (AGB). At each year, data are averages of all the 1km×1km grids (a) and across a certain grassland type at the regional scale (b, c and d).